Available online at www.sciencedirect.com
SCIENCE DIRECT
Catalysis Today 110 (2005) 281–293
CATALYSIS TODAY
www.elsevier.com/locate/cattod

A new insight in the unusual adsorption properties of Cu^+ cations in Cu-ZSM-5 zeolite

V.B. Kazansky, E.A. Pidko *

N.D. Zelinsky Institute of Organic Chemistry of Russian Academy of Sciences, Leninsky Prospect 47, Moscow 119991, Russia

Available online 24 October 2005

Abstract

ZSM-5 zeolites modified with Cu^+ ions were prepared either by the high-temperature chemical reaction of hydrogen form with CuCl vapour or by the wet ion exchange with subsequent reduction of the modified samples in CO at 873 K. Adsorption of H_2, N_2 or C_2H_6 by Cu^+ ions was studied by DRIFTS and by volumetric technique. The conclusions about the structure of adsorption complexes were supported by the DFT cluster quantum chemical calculations. The obtained results indicated that in addition to the previously reported strong adsorption of nitrogen, the univalent copper also unusually strongly adsorbs molecular hydrogen and ethane. Adsorption of hydrogen is the most amazing since the observed low-frequency shifts of the H–H stretching vibrations were as high as about 1000 cm^{-1}. This is quite different from much weaker H_2 perturbation by Cu^{2+} cations. Adsorption of ethane by Cu^+ ions also resulted in the low-frequency shifts of some of C–H IR stretching bands up to 400 cm^{-1}. The DFT cluster modelling indicated that both adsorption of hydrogen and ethane could be explained by interaction with the isolated Cu^+ ions localized at the α sites of the ZSM-5 framework. Quantum chemical calculations indicated the important role in the bonding of adsorbed hydrogen and ethane of electron back donation from d_π-orbitals of Cu^+ ions to the σ^*H–H or C–H orbitals. The overall yield of Cu^+ sites of the strong H_2 or N_2 adsorption is about twice lower than the total copper content.

Keywords: CuZSM-5; Dihydrogen adsorption; Ethane adsorption; DRIFTS; DFT; Light alkane transition metal complexes

1. Introduction

The copper modified ZSM-5 zeolits (CuZSM-5) are known to exhibit a high-catalytic activity in selective decomposition of NO into molecular oxygen and nitrogen [1–3]. They also possess very unusual adsorption properties, resulting in formation of a very strong adsorption complexes of the univalent copper cations with N_2 [4,5] or CO molecules [6]. The Cu^+ adsorption centers could be formed both in an indirect way via reduction of dimeric oxygen-bridged $[Cu–O–Cu]^{2+}$ species in CO or directly by high-temperature reaction of the hydrogen form with CuCl vapour at elevated temperature [4,7–9].

Earlier in our works [10–19], low-temperature dihydrogen adsorption has been suggested as a very sensitive tool for the study of different cationic sites in the zeolites. The values of the low-frequency shifts of the IR H–H stretching bands were used in this case as a measure of the polarizing ability of cations. It was demonstrated that adsorption of H_2 by alkaline or alkali-earth cations results in a rather weak perturbation of adsorbed molecules, while the red shifts of H–H stretching bands, usually do not exceed 100–150 cm^{-1}. In contrast, such strong Lewis acid sites as Zn^{2+} or Cd^{2+} cations stabilized in the structure of high-silica zeolites perturb adsorbed H_2 much stronger [17–19]. In this case, the low-frequency shifts are as high as 220 cm^{-1}. This testifies a very strong polarization of the H–H bond that results in subsequent heterolytic dissociative adsorption of hydrogen at elevated temperatures. However, in all these cases adsorption heats were relatively low, since the study of H_2 adsorption was possible only at liquid nitrogen temperature. In contrast, hydrogen adsorption, that was recently reported in refs. [20,21] for the reduced over-exchanged CuZSM-5 zeolite, is quite different. It results in low-frequency shifts of the H–H stretching vibrations by about 1000 cm^{-1}. Such large shifts have never been reported before for H_2 adsorbed by any oxide

* Corresponding author. Present address: Schuit institute of Catalysis, Eindhoven University of Technology, P.O. Box 513, 5600 MB Eindhoven, The Netherlands.
E-mail address: e.pidko@tue.nl (E.A. Pidko).

0920-5861/$ – see front matter © 2005 Elsevier B.V. All rights reserved.
doi:10.1016/j.cattod.2005.09.037

or any cationic form of zeolite. Similar results were also obtained for H_2 adsorption by CuZSM-5 prepared via high-temperature reaction with CuCl vapour [22,23].

On the other hand, during last 20 years, a great number of transition metal complexes containing intact molecular dihydrogen have been reported [24–32]. These systems constitute a special class of σ-bond complexes. The vibrational properties of the M–H_2 moiety in such σ-bonded hydrogen complexes were discussed in refs. [25–27,30]. They are very similar to those observed in refs. [20–23] for H_2 adsorption by CuZSM-5 zeolite. Therefore, it is most likely, that the bonding of adsorbed H_2 with Cu^+ could be described in the similar way. Indeed, analysis of the components of adsorption energy of H_2 by Cu^+ cations, carried out within the cluster approach by Solans-Monfort et al. [22], revealed the σ-bonding of adsorbed hydrogen. In this case, the electron donation from the $H_2(\sigma_g)$ bonding orbital to the low-occupied Cu(4s) orbital is combined with the electron back-donation from the $(3d_\pi)$ Cu^+ orbital to the antibonding $H_2(\sigma_u^*)$ orbital, while the orbital polarization plays a significant role in the H_2 adsorption energy. This causes the above-mentioned very large batochromic H–H frequency shifts.

Our recent investigations of hydrogen and light alkanes adsorption by different cationic forms of zeolites [10–19,33–35] also showed, that the ion exchanged transition metal cations usually exhibit very similar adsorption properties with respect both to H_2 and light paraffins (see, for instance, refs. [19,34]). However, most of these works were aimed on the study of interaction of adsorbed molecules with the strong Lewis acids when no donor–acceptor complexes were formed upon adsorption. Therefore, in the present work, we carried out the parallel IR study of molecular hydrogen and ethane adsorption by Cu^+ ions in CuZSM-5 zeolites with different Si/Al ratio in the framework. DFT modelling of adsorption complexes was also carried in parallel in order to analyze hydrogen and ethane bonding with Cu^+ ions stabilized in the zeolite lattice.

In this connection one should note, that despite numerous observations of H_2 σ-complexes [36,37], no similar series of the stable complexes with transition metals have been previously reported for light alkanes. All of the alkane complexes so far detected are unstable at room temperature and rather specific methods are required for their preparation and detection.

Indeed, the first examples of alkane coordination by transition metals were reported upon application of the matrix isolation technique in the photochemistry of the d^6 $M(CO)_6$ carbonyls (M=Cr, Mo, W) [38,39]. The coordination of alkanes to $M(CO)_5$ fragment has also been observed by transient absorption technique in solution or in the gas phase in refs. [40–42]. More recently, the coordination of methane by the naked transition metal atoms has been directly observed in the low-temperature matrices. Experiments on the oxidative addition and reductive elimination of alkanes from transition metal complexes also revealed the formation of alkane complexes as reaction intermediates [37,43]. The complexes with light alkanes have been also subjected to theoretical calculations in refs. [37,44], both as intermediates in C–H activation, or as the independent entities. However, direct observation of these species has not been reported yet.

2. Experimental

Initial hydrogen forms of SN-55 or SN-300 ZSM-5 zeolites from ''Alsi Penta'' with Si/Al ratio in the framework of about 22 and 150, respectively, were prepared by decomposition of the corresponding ammonium forms in flowing oxygen at 773 K. Modification of the zeolites with the univalent copper was carried out either via reduction of dimeric oxygen-bridged $[Cu–O–Cu]^{2+}$ species prepared by the wet ion over exchange or directly by the reaction of the hydrogen form with CuCl vapour at high temperature. In the latter case a high Si/Al ratio of 150 was chosen in order to minimize the interaction between copper species inside the zeolite channels, which could lead to formation of bivalent copper cations via the following disproportion reaction:

$$2Z^-Cu^+ \rightarrow Cu^0 + Z^-Cu^{2+}Z^- \quad (1)$$

The ion-exchanged copper containing (Cu/H-ZSM-5_{red}) samples were prepared by triple wet ion exchange of the ammonium form of the SN-55 zeolite (Si/Al = 22) with 0.02 M copper acetate aqueous solution. After third exchange the material was washed in distilled water and dried at 380 K. According to the atomic absorption spectral analysis (AAS), the copper content in the sample was equal to 2.5 wt.%. This value corresponds to Cu/Al ratio of 0.6. Calcination and reduction treatments of the modified samples were performed under static conditions directly in the IR cell. The calcination was carried out in oxygen at the pressure of 13.3 kPa at 773 K for 1 h. The reduction in CO was performed at 873 K for three times (each time for 0.5 h) in the static conditions at the CO pressure of 13.3 kPa (the Cu/H-ZSM-5_{red} sample).

The Cu(I)-ZSM-5 sample was prepared directly by reaction of HZSM-5 with the CuCl vapour at 573 K following the procedure previously described in ref. [8]. This was done in the same quartz optical cell that was subsequently used for DRIFTS measurements. For this purpose, the optical cell was equipped with a side arm with CaF_2 window and an appendix, containing CuCl (Merck) that was previously evacuated at 473 K in order to remove any traces of water. At first, the zeolite was heated in vacuum at 393 K for 2 h with the rate of preliminary temperature increase of 2 K/min. Then the temperature was raised with the same heating rate to 773 K and the samples were evacuated at this temperature for two more hours. After that HZSM-5 was transferred into the appendix with CuCl and heated in vacuum at 573 K. At the end of HCl evolution the modified zeolite was transferred back into the main part of the quartz cell and was evacuated for two more hours at 773 K in order to remove the excess of the copper chloride.

H_2 and N_2 adsorption was studied for both Cu/H-ZSM-5 and Cu(I)-ZSM-5 samples, whereas DRIFT study of C_2H_6 adsorption was performed only for the sample prepared via high-temperature reaction with copper(I) chloride.

Diffuse-reflectance (DRIFT) and transmittance IR measurements were carried out using a Nicolet ''Impact 410''

spectrophotometer equipped with a home-made diffuse reflectance attachment. The DRIFTS measurements were preformed for the granulated zeolites with dimensions of grains of ca. 0.2–0.5 mm. The spectra of adsorbed N_2 and C_2H_6 were recorded at room temperature trough a CaF_2 window, while those of adsorbed hydrogen either at room temperature or at 77 K. In the latter case, the quartz optical sell was immersed into a quartz Dewar flask filled with liquid nitrogen. All of the spectra were transformed into Kubelka–Munk units by a standard program assuming that the reflectance ability of the samples at 5000 cm^{-1} was equal to 0.9. Then the background created by the zeolite was subtracted from the overall spectra. The transmittance measurements were performed for the self-supported pellets pressed from the zeolite powders also using the quartz IR cell with CaF_2 windows.

The numbers of sites of strong H_2 and N_2 adsorption were evaluated from adsorption isotherms of both these gases, which were measured volumetrically at 293 K. It was accepted that at room temperature adsorption of molecular hydrogen by the residual acidic hydroxyls or by Lewis Al^{3+} sites was very weak and did not contribute into adsorption of H_2 by the Cu^+ ions. Their number was estimated by extracting of the Langmuir parts from the entire adsorption isotherms.

The quantum chemical calculations were carried out within the gradient-corrected density functional theory (DFT) using the GAUSSIAN-98 program [45]. The hybrid B3LYP [46] functional was used in these calculations, since it gives acceptable values for molecular energies and geometries [47]. All of the calculations were performed using standard 6–31 G (d, p) basis set for all atoms of the cluster modelling the adsorption site and for the adsorbed C_2H_6, N_2 or H_2 species.

The six-membered ring composed of two five-membered rings from the walls of the straight channels of the ZSM-5 zeolite (the α-site) was chosen as a possible site both for Cu^+ and Cu^{2+} localization. This model was selected since it has been discussed by experimentalists to explain unusual catalytic and chemical properties of univalent copper exchanged into high-silica zeolites [48]. Using the QM-pot approach, Nachtigallova et al. [49] have also shown theoretically that this site is among the most stable for the Cu^+ localization. The DFT modelling was performed for the $CuAlSi_6O_8H^*_{12}$ clusters, with Al atoms placed in either T2 (Fig. 1(a)), T1 (Fig. 1(b)) or T4 (Fig. 1(c)) lattice positions. Below these structures will be designated as $Cu^+Z_I^-$, $Cu^+Z_{II}^-$ and $Cu^+Z_{III}^-$, respectively. For modelling of the Cu^{2+} at the α-site of ZSM-5 the $CuAlSi_5O_8H^*_{12}$ cluster ($Cu^{2+}Z^{2-}$, Fig. 1(d)) was used.

To saturate the dangling Si–O bonds at the borders of these clusters hydrogen atoms were used. By analogy with ref. [50], special restrictions were imposed on the procedure of optimization of their positions. At first, the structure of initial zeolite cluster was constrained according to the X-ray diffraction data [51]. Then only Si–H^* and Al–H^* bond lengths and position of the copper ion were optimized, while positions of other atoms as well as directions of the chemical bonds were fixed according to crystallographic data. The copper cation was allowed to move freely. The positions of H^* atoms in all subsequent calculations were then fixed, while those of the remaining atoms of the cluster were optimized.

The calculated adsorption energies were corrected for the zero-point energies (ZPE) obtained from the vibrational mode calculations, whereas the correction for the basis set super-

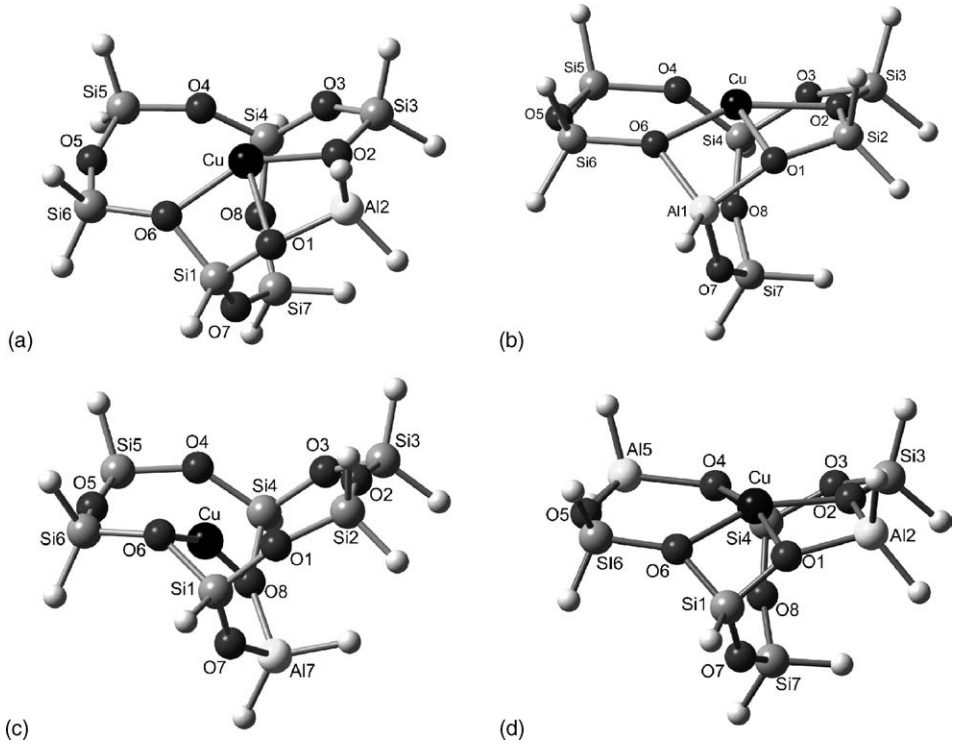

Fig. 1. Optimized structures of (a) $Cu^+Z_I^-$, (b) $Cu^+Z_{II}^-$, (c) $Cu^+Z_{III}^-$ and (d) $Cu^{2+}Z^{2-}$ clusters.

position error (BSSE) was not included due to very significant changes of the optimized clusters geometry after adsorption.

To investigate the orbital distribution of electrons and to estimate the energies of donor–acceptor interactions in the ethane adsorption complexes with Cu^+ ions, the population analysis was performed using Natural Bond Orbital method program that has been attached to the GAUSSIAN-98 package. According to the ref. [52], this method allows a rather reasonable description of different types of interatomic interactions and discrimination of their types, as well as analysis of the orbital populations and orbital energies.

3. Results and discussion

3.1. DRIFTS and volumetric study of H_2 adsorption by ZSM-5 zeolites modified by wet ion exchange or by high-temperature reaction with CuCl vapour

DRIFT spectra of OH groups in the initial hydrogen form of ZSM-5 with Si/Al = 22 or in the zeolite modified with copper by wet ion-exchange from the aqueous solution of $Cu(OAc)_2$ with subsequent reduction in CO at 873 K (Cu/H-ZSM-5_{red}) are shown in Fig. 2(a and b), respectively. In agreement with the literature data [18], both of them contain the narrow band at 3610 cm^{-1} from the isolated acidic hydroxyl groups and a much weaker band with the maximum at 3740 cm^{-1} from the silanol groups. A very broad band with the maximum at ~2900–3600 cm^{-1} also belongs to the acidic OH groups, which are hydrogen-bonded to the basic oxygen atoms of the zeolite framework.

DRIFT spectra in Fig. 2 indicated that the wet ion-exchange resulted in substitution of about 60% of protons by copper. On the other hand, according to the AAS analysis the copper content in the Cu/H-ZSM-5 sample was equal to 2.5 wt.%. For the zeolite with the Si/Al ratio of 22 this value just corresponds to substitution by Cu^+ ions of about 60% of OH groups. In contrast, substitution of 60% of OH groups with bivalent copper cations should result in a twice lower copper loading, i.e. only of 1.25 wt.%. Therefore, there is no doubt that after reduction in CO, the predominant part of copper in the ion-exchanged sample was transformed into Cu^+ cations. This conclusion well

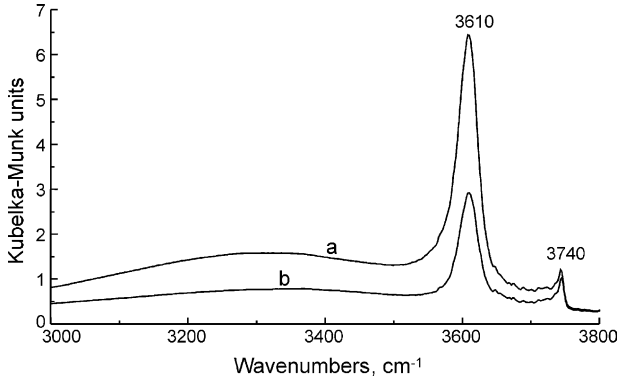

Fig. 2. DRIFT spectra of OH groups in HZSM-5 (Si/Al = 22) (a) and in the copper modified zeolite after reduction in CO at 873 K (Cu/H-ZSM-5_{red}) (b). DRIFT measurements at room temperature.

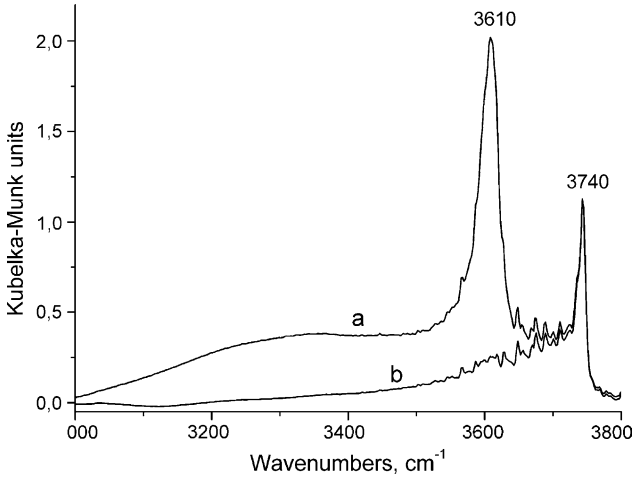

Fig. 3. DRIFT spectra of OH groups in the initial HZSM-5 (Si/Al = 150) (a) and after reaction with CuCl at 573 K and subsequently evacuated at 773 K (Cu(I)-ZSM-5) (b). DRIFT measurements at room temperature.

agrees with the previously reported literature data on reduction of bivalent copper in CO or on its self-reduction after vacuum treatment at high temperature [5,6,53–55].

As follows from Fig. 3, the reaction of HZSM-5 with CuCl at 573 K with subsequent evacuation of the sample at 773 K resulted in quantitative substitution of all acidic protons by the univalent copper ions. Indeed, such pretreatment completely destroyed both the narrow OH-band at 3610 cm^{-1} and the broad band in the region of ~2900–3600 cm^{-1}. In contrast, the silanol groups were not involved in the reaction with copper chloride, since the intensity of the band at 3740 cm^{-1} did not change.

Fig. 4(a–d) shows DRIFT spectra of hydrogen adsorbed at 77 K by the Cu/H-ZSM-5 sample after different pretreatments. The band at 4105 was earlier reported for low-temperature H_2 adsorption on the non-modified HZSM-5 [17,18]. Therefore, it belongs to H_2 adsorption by the residual acidic OH groups. A

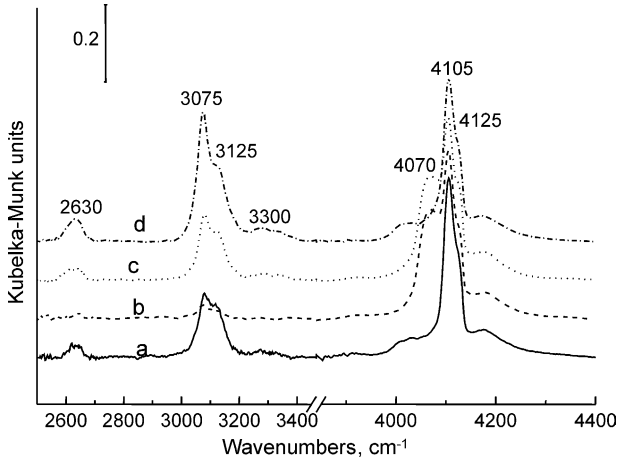

Fig. 4. DRIFT spectra of molecular hydrogen adsorbed by the Cu/H-ZSM-5 sample at 77 K at the pressure of 13.3 kPa after different pretreatments: (a) the sample pre-reduced in CO was evacuated for 2 h at 873 K; (b) sample (a) was calcinated in oxygen at 773 K and evacuated at RT; (c) sample (b) was evacuation at 873 K; (d) sample (c) was reduced in CO at 600 °C and then evacuated at this temperature. DRIFT measurements at 77 K.

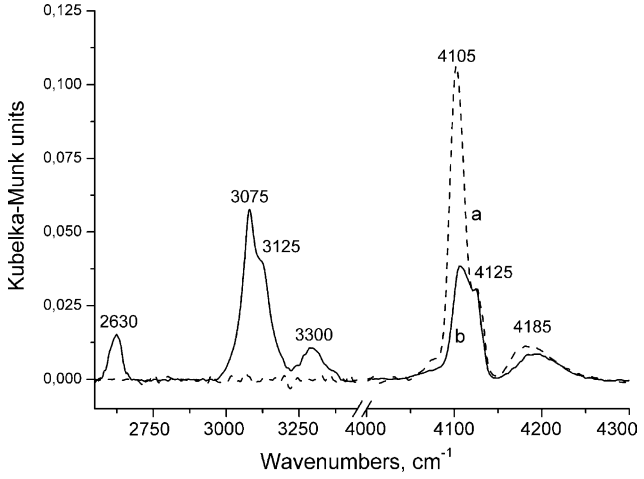

Fig. 5. DRIFT spectra of H_2 adsorbed at 77 K at the pressure of 13.3 kPa by the parent HZSM-5 with Si/Al = 150 (a) and after modification with copper(I) chloride (b). DRIFT measurements at 77 K.

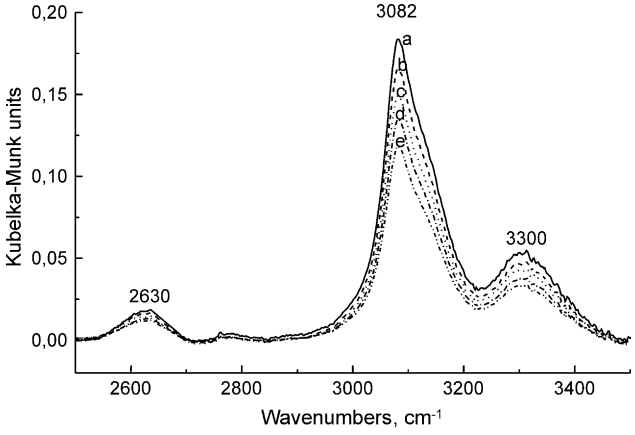

Fig. 6. DRIFT spectra of molecular hydrogen adsorbed at room temperature at different pressures by the Cu/H-ZSM-5_{red} sample: (a) 26.6 kPa, (b) 13.3 kPa and (c) 6.7, 3.3 and 1.3 kPa. DRIFT measurements at room temperature.

much weaker band at 4175 cm^{-1} corresponds to the high-frequency satellite of the band at 4105 cm^{-1}, while the broad band at 4030 cm^{-1} is due to hydrogen adsorption by the Lewis acid sites formed due to partial dehydroxylation of the zeolite upon high-temperature vacuum pretreatment [17].

The low-frequency bands at 3075, 3125, 3300 and 2630 cm^{-1} are connected with hydrogen adsorption by Cu^+ ions. One should note that such dramatic low-frequency shifts of H–H stretching vibrations indicate a very strong perturbation of adsorbed H_2. The similar low values of H–H stretching vibrational frequencies have been observed only for transition metal dihydrogen complexes in solutions [25–27,30] or for CuCl complex with H_2 stabilized in the argon matrix [56] and were never reported for H_2 adsorbed by any cation exchanged zeolite or oxide.

The reduced copper sites of the strong perturbation of adsorbed hydrogen can be easily destroyed by calcinations of the sample in oxygen at 873 K. As follows from Fig. 4(b), such treatment results in almost complete disappearance of all low-frequency H–H stretching bands. Instead a new band appeared at 4070 cm^{-1} that, most likely, belongs to H_2 adsorbed by [Cu^{2+}–O–Cu^{2+}] oxo-species formed via oxidation of two adjacent Cu^+ cations. Evacuation of the oxidized sample at 873 K (Fig. 4(c)) partially restores the intensity of the low-frequency bands most likely due to destruction of the oxo-species. Subsequent reduction in CO leads to the further increase of the low-frequency bands of adsorbed hydrogen in intensity. The simultaneous elimination of the band at 4070 cm^{-1} (Fig. 4(d)) testifies subsequent reduction of the oxo-bridging copper species.

In the similar way, a set of the low-frequency bands at 3075, 3125, 3300 and 2635 cm^{-1} also appeared upon hydrogen adsorption on the Cu(I)-ZSM-5 sample with Si/Al = 150 (Fig. 5). As already indicated above, the band of adsorbed hydrogen at 4105 cm^{-1} usually is ascribed to interaction with acidic OH groups. However, as follows from Fig. 3(b), all of them were destroyed in the Cu(I)-ZSM-5 zeolite by reaction with CuCl vapour. Therefore, instead, this band should be rather ascribed to H_2 molecules only slightly perturbed via adsorption by some inactive copper species, while the H–H stretching frequency of adsorbed hydrogen occasionally coincided in this case with that for adsorption on acidic protons.

Anyway, these results definitely indicate that the unusually strongly low-frequency shifted DRIFT bands belong to hydrogen molecules, which are very strongly perturbed by interaction with Cu^+ cations. The amazing feature of this unusual form of hydrogen adsorption is that both for Cu/H-ZSM-5_{red} and Cu(I)-ZSM-5 samples the corresponding DRIFTS bands are observed even at room temperature (Figs. 6 and 7, respectively), while for both these zeolites the positions of the bands of hydrogen adsorbed at room temperature and at 77 K are very close to each other.

For the Cu/HZSM-5_{red} sample prepared via wet ion exchange we also recorded the transmittance IR spectrum of hydrogen adsorbed at room temperature (Fig. 8). This allowed observation of additional bands at lower frequencies with maxima at 1395 and 1810 cm^{-1}. Similar to the other bands of

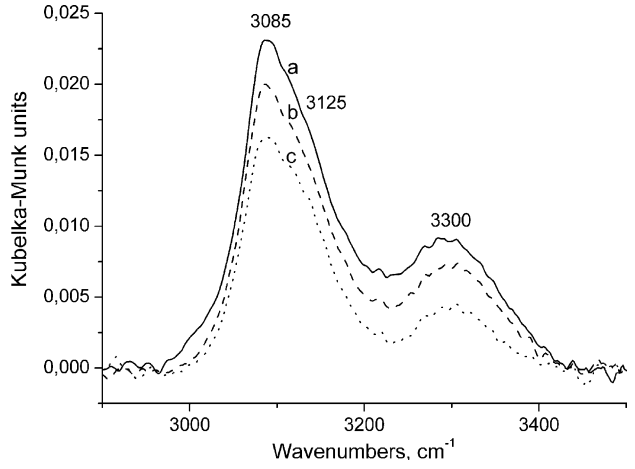

Fig. 7. DRIFT spectra of H_2 adsorbed by the Cu(I)-ZSM-5 sample at room temperature and at different equilibrium pressures: (a) 40 kPa, (b) 26.6 kPa and (c) 13.3 kPa. DRIFT measurements at room temperature.

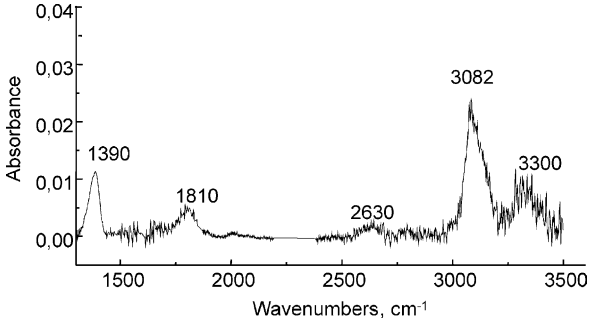

Fig. 8. Transmittance IR spectrum of H_2 adsorbed by Cu/H-ZSM-5_{red} at room temperature at the equilibrium pressure of 6.7 kPa.

adsorbed hydrogen, both of them can be removed by evacuation at room temperature. Therefore, they definitely belong to the same adsorbed species as the rest of DRIFT bands of adsorbed hydrogen.

By analogy with the vibrational spectra of the transition metal dihydrogen complexes [25–27,30], we ascribe the band at 1395 cm^{-1}, to the symmetric vibration of the CuH_2 moiety, relative to Cu^+ ions, while the band at 1810 cm^{-1} to the corresponding asymmetric vibration that changes orientation of hydrogen molecule relative to the adsorption site (Fig. 9). Similar to ref. [22] we also ascribe the bands at 3082 and 3125 cm^{-1} to the H–H stretching vibrations of the very strongly perturbed H_2 molecules adsorbed by Cu^+ cations. The more convincing arguments for such assignments will be provided by results of our DFT modelling of adsorption complexes, we discuss in the next paragraph.

To evaluate the number of the sites of the strong dihydrogen adsorption, we measured hydrogen adsorption isotherms The obtained results indicated that for the Cu/H-ZSM-5_{red} sample the fraction of Cu^+ sites strongly adsorbing H_2 molecules corresponds to about 0.45 of the total copper content, while for the sample prepared by the high-temperature reaction with CuCl vapour to about 0.37 (see Table 1). We also found that both for the Cu/H-ZSM-5_{red} and for the Cu(I)-ZSM-5 samples the preliminary nitrogen adsorption at room temperature eliminated the DRIFT bands of adsorbed hydrogen. Therefore, one can conclude that the sites of both the stronger nitrogen adsorption and the weaker hydrogen adsorption are the same Cu^+ ions.

On the other hand, only about twice lower amounts of hydrogen and nitrogen adsorption in comparison with the total copper content, indicate that about one-half of the modifying

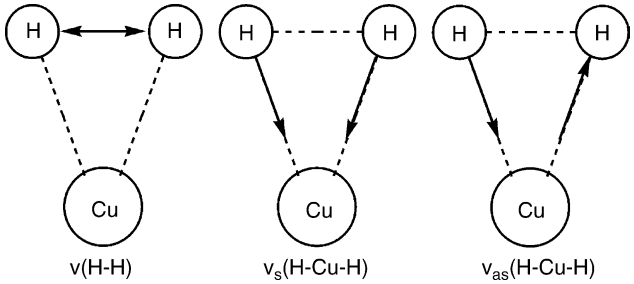

Fig. 9. Vibrational modes of CuH_2 moiety of the H_2 adsorption comlex with Cu^+ cation.

Table 1
Molar ratios of uptake of H_2 and N_2 to the copper content in CuZSM-5

	H_2/Cu	N_2/Cu
Cu/H-ZSM-5_{red}	0.45	0.55
Cu(I)-ZSM-5	0.37	0.46

Cu^+ ions are accessible for both N_2 and H_2 molecules. Moreover, about 20% of the Cu^+ sites of the strong dinitrogen adsorption are inactive with respect to hydrogen adsorption. This indicates that the Cu^+ cations are strongly inhomogeneous and exhibit different adsorption properties. Such inhomogenity could be explained by different coordination and accessibility or by different binding properties of univalent copper depending on different localization in the ZSM-5 framework.

3.2. The DFT cluster modelling of H_2 and N_2 adsorption by Cu^+ cations stabilized at the α-position of ZSM-5 zeolite

In order of more convincing assignment of the above presented spectral results, we performed the DFT modelling of N_2 and H_2 adsorption by Cu^+ cations stabilized in three different clusters (Fig. 1(a–c)). Their geometry is similar to that one of α-sites in ZSM-5 zeolite, but the clusters differ in localization of aluminium atoms. The optimized Cu–O bond lengths obtained by these calculations are summarized in Table 2.

As one could expect, the copper cations are localized in $Cu^+Z_I^-$ and $Cu^+Z_{II}^-$ clusters more closely to Al atoms. Therefore, despite of the effective coordination number of Cu^+ by the zeolitic oxygen atoms equal to 3, the bond lengths with two oxygen atoms adjacent to the aluminium are somewhat shorter compared with the third Cu–O bond. In contrast, for the $Cu^+Z_{III}^-$ cluster the copper cation is very strongly shielded by the surrounding relatively closely located O4, O5 and O7 atoms. The calculated structures of dihydrogen adsorption complexes with Cu^+ cation for $Cu^+Z_I^-$, $Cu^+Z_{II}^-$ and $Cu^+Z_{III}^-$ clusters are shown in Fig. 10(a–c), respectively, while Table 3 documents the H_2 adsorption energies, the calculated H–H stretching frequencies and the interatomic distances of the Cu–H_2 moiety.

The obtained results indicated that adsorption of H_2 by all three clusters via the end-on (η^1) adsorption fashion is non realistic, since optimization of geometry leads to formation of η^2-adsorption σ-complexes. The calculations also indicated, that adsorption of H_2 by both $Cu^+Z_I^-$ and $Cu^+Z_{II}^-$ clusters is much stronger (15.49 and 20.83 kcal/mol, respectively) than by the $Cu^+Z_{III}^-$ cluster (0.83 kcal/mol). This results in the considerable elongation of the H–H bond in comparison with the free H_2 molecule and, thereupon, in a very large batochromic shifts of the corresponding stretching frequencies. The calculated adsorption heats testify formation of the rather strong donor–acceptor [$Cu^+(\eta^2$-$H_2)$] complexes and are in a good agreement with the previously reported theoretical results obtained by Solans-Monfort et al. [22].

The calculated frequencies are also in a good agreement with the above-discussed experimental data and permit a more precise assignment of DRIFT bands of adsorbed hydrogen.

Table 2
The optimized Cu–O bond lengths in $Cu^+Z_I^-$, $Cu^+Z_{II}^-$, $Cu^+Z_{III}^-$ and $Cu^{2+}Z^{2-}$clusters before and after adsorption of H_2, N_2 or C_2H_6 (Å)

	$Cu^+Z_I^-$	$Cu^+Z_{II}^-$	$Cu^+Z_{III}^-$	$Cu^{2+}Z^{2-}$	$H_2/Cu^+Z_I^-$	$H_2/Cu^+Z_{II}^-$	$H_2/Cu^+Z_{III}^-$	$H_2/Cu^{2+}Z^{2-}$
Cu–O1	2.051	2.041	3.094	2.003	2.055	1.986	2.403	2.006
Cu–O2	1.927	2.272	3.507	1.998	2.011	3.118	2.136	2.000
Cu–O3	3.171	3.005	3.262	3.201	3.485	3.871	2.874	3.206
Cu–O4	2.956	2.765	2.421	2.022	3.322	3.515	2.848	2.028
Cu–O5	3.683	3.709	2.480	3.634	3.986	3.761	3.263	3.638
Cu–O6	2.229	1.921	1.921	2.056	2.447	1.917	2.108	2.059
Cu–O7	3.274	3.301	2.408	3.164	3.770	3.982	2.883	3.176
Cu–O8	3.128	3.020	1.881	2.911	3.650	4.094	2.026	2.944

	$N_2/Cu^+Z_I^-$	$N_2/Cu^+Z_{II}^-$	$N_2/Cu^+Z_{III}^-$	η^1-$C_2H_6/Cu^+Z_{II}^-$	η^2-$C_2H_6/Cu^+Z_{II}^-$
Cu–O1	2.060	2.020	2.648	2.226	2.076
Cu–O2	2.011	3.049	2.745	2.141	3.202
Cu–O3	3.363	3.777	2.932	3.130	4.151
Cu–O4	3.379	3.413	2.463	2.913	3.745
Cu–O5	4.115	3.741	2.953	3.744	3.850
Cu–O6	2.574	1.935	2.037	1.654	1.938
Cu–O7	3.833	3.978	3.344	3.519	4.083
Cu–O8	3.790	4.023	2.185	3.272	4.331

Similar to ref. [22] we attribute the bands at 3075 and 3125 cm^{-1} to the H–H stretching vibrations of hydrogen adsorbed by the isolated Cu^+ cations in the $Cu^+Z_I^-$ and $Cu^+Z_{II}^-$ clusters. The band at 1395 cm^{-1} most likely belongs to the symmetric vibration of the H_2 molecule relative to adsorption site as a whole. Respectively, the band at 1810 cm^{-1} is most likely due to the asymmetric Cu–H_2 bending vibration that changes orientation of adsorbed hydrogen (Fig. 9). The weaker band at 2630 cm^{-1} could be ascribed to the overtone of the band at 1390 cm^{-1} from the symmetric Cu–H_2 vibrations. The assignment of the band at 3300 cm^{-1} at present is still disputable. Solans-Monfort et al. [22] supposed that this band belongs to H_2 adsorbed by residual CuCl. However, the present experimental data shows that it is observed both for the sample

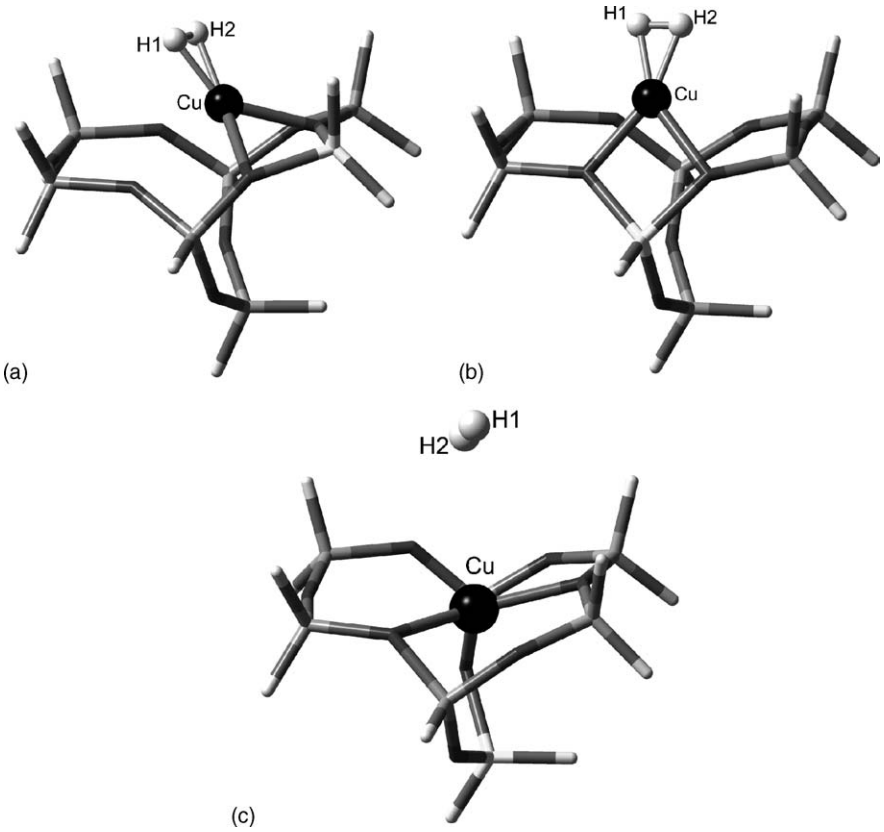

Fig. 10. Adsorption of H_2 by Cu^+ cations stabilized at (a) $Cu^+Z_I^-$, (b) $Cu^+Z_{II}^-$ and (c) $Cu^+Z_{III}^-$ clusters.

Table 3
Clauculated H_2 and N_2 adsorption energy (kcal/mol), H–H and N–N harmonic stretching frequencies (cm^{-1}) and bond lengths (Å) of the CuH_2 and the CuN_2 moiety for H_2 and N_2 molecules adsorbed by clusters $Cu^+Z_I^-$, $Cu^+Z_{II}^-$, $Cu^+Z_{III}^-$ and $Cu^{2+}Z^{2-}$

	Free H_2	$H_2/Cu^+Z_I^-$	$H_2/Cu^+Z_{II}^-$	$H_2/Cu^+Z_{III}^-$	$H_2/Cu^{2+}Z^{2-}$
l(H–H)	0.730	0.834	0.859	0.744	0.745
l(Cu–H)	–	1.569, 1.576	1.545, 1.542	3.342, 3.490	2.830, 2.837
Eads	–	15.49	20.83	0.83	1.05
ν(H–H)	4465	3125	2829	4428	4401
ν_s(Cu–H_2)	–	1173	1240	152	188
ν_{as}(Cu–H_2)	–	1594	1757	288	291

	Free N_2	$N_2/Cu^+Z_I^-$	$N_2/Cu^+Z_{II}^-$	$N_2/Cu^+Z_{III}^-$
l(N–N)	1.106	1.114	1.115	1.113
l(Cu–N)	–	1.786	1.763	1.826
E_{ads}	–	26.63	29.83	15.41
ν(N–N)	2457	2361	2361	2363

prepared via high-temperature reaction of HZSM-5 with copper(I) chloride and for the wet ion-exchanged sample. Therefore, we suggest that this band belongs to H_2 adsorbed by the exchanged Cu^+ cations.

One can also emphasize that formation of the [$Cu^+(\eta^2$-$H_2)$] adsorption complexes leads to the significant changes in the geometry of the adsorption sites. For both $Cu^+Z_I^-$ and $Cu^+Z_{II}^-$ clusters the Cu^+ ion partially leaves the initial cationic site upon hydrogen adsorption, while its coordination number to the lattice oxygen atoms becomes equal to 2. In contrast, adsorption of hydrogen by Cu^+ cation in the $Cu^+Z_{III}^-$ cluster that is strongly shielded with the surrounding lattice oxygens results neither in any significant perturbation of H_2 molecule, nor in the change of the adsorption site geometry (Tables 2 and 3). Indeed, the calculated H–H bond length increased in this case only by 2%, while the H–H stretching frequency decreased in comparison with the free H_2 less than by 1% (Table 3). The calculated adsorption energy is also very low (only 0.83 kcal/mol).

In the similar way, according to the DFT modelling, H_2 adsorption by the bivalent copper in $Cu^{2+}Z^{2-}$ (Fig. 11) cluster also does not lead to any significant changes of this adsorption site in the geometry (Table 2). The changes, which occur in the H_2 moiety, are also very minor: the length of the H–H bond increased only by 2% in comparison with the similar value calculated for the free H_2 molecule, while the H–H frequency decreased less than by 2% (Table 3). In this case, adsorption most likely results from polarization of hydrogen by the electrostatic field of Cu^{2+} cation, while the copper-to-hydrogen back donation is very unlikely.

Similar to H_2 adsorption, we also performed the DFT modelling of N_2 adsorption by Cu^+ cations in the same $Cu^+Z_I^-$, $Cu^+Z_{II}^-$ or $Cu^+Z_{III}^-$ clusters. In agreement with the earlier published results [4,5], we concluded that N_2 is adsorbed via end-on fashion. The calculated adsorption structures are presented in Fig. 12(a–c), while Table 3 documents the N_2 adsorption energies, the calculated N–N stretching frequencies and the interatomic distances of the Cu–N_2 moiety. The obtained values are in a reasonably good agreement with the previously reported experimental and theoretical data [4–5,11–12]. However, unlike for H_2, the N_2 adsorption energies for all of these clusters are considerably higher and do not so strongly depend on positions of Al atoms in the clusters. Moreover, the values of the N–N stretching frequencies for all these structures are very close to each other. We suggest that more strong adsorption of N_2 compared to H_2 adsorption results in less sensitivity of nitrogen as a molecular probe.

Thus, the results of our DFT modelling explain inhomogeneity of Cu^+ adsorption sites even for the simplest example of α-sites with different localization of aluminum atoms. These sites certainly correspond only to one of the possibilities of copper localization. However, even this simplest model illustrates the possible origin of inhomogeneity. We also suggest that the Cu^+ sites of the stronger N_2 adsorption, which are inactive with respect to adsorbed H_2 molecules could be strongly shielded with the surrounding oxygen atoms Cu^+ ions. Most likely, that the band at 4105 cm^{-1} in the DRIFT spectra of hydrogen adsorbed by Cu(I)-ZSM-5 (Fig. 12(b)) belongs just to such sites.

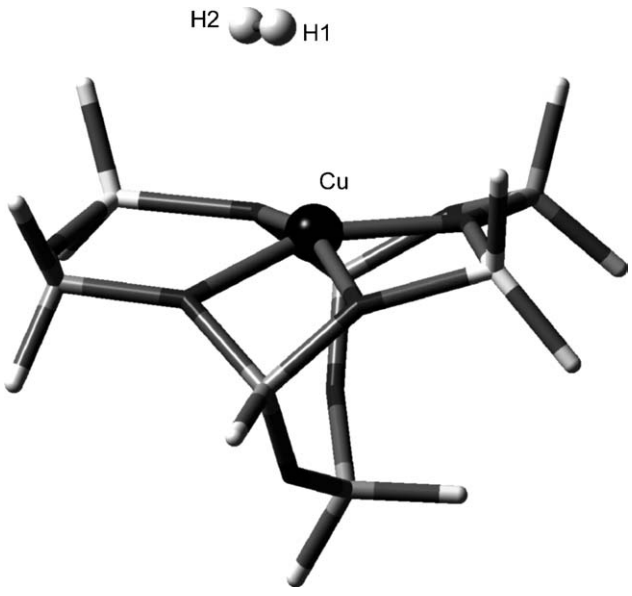

Fig. 11. Adsorption of H2 by Cu^{2+} cation stabilized at $Cu^{2+}Z^{2-}$ cluster.

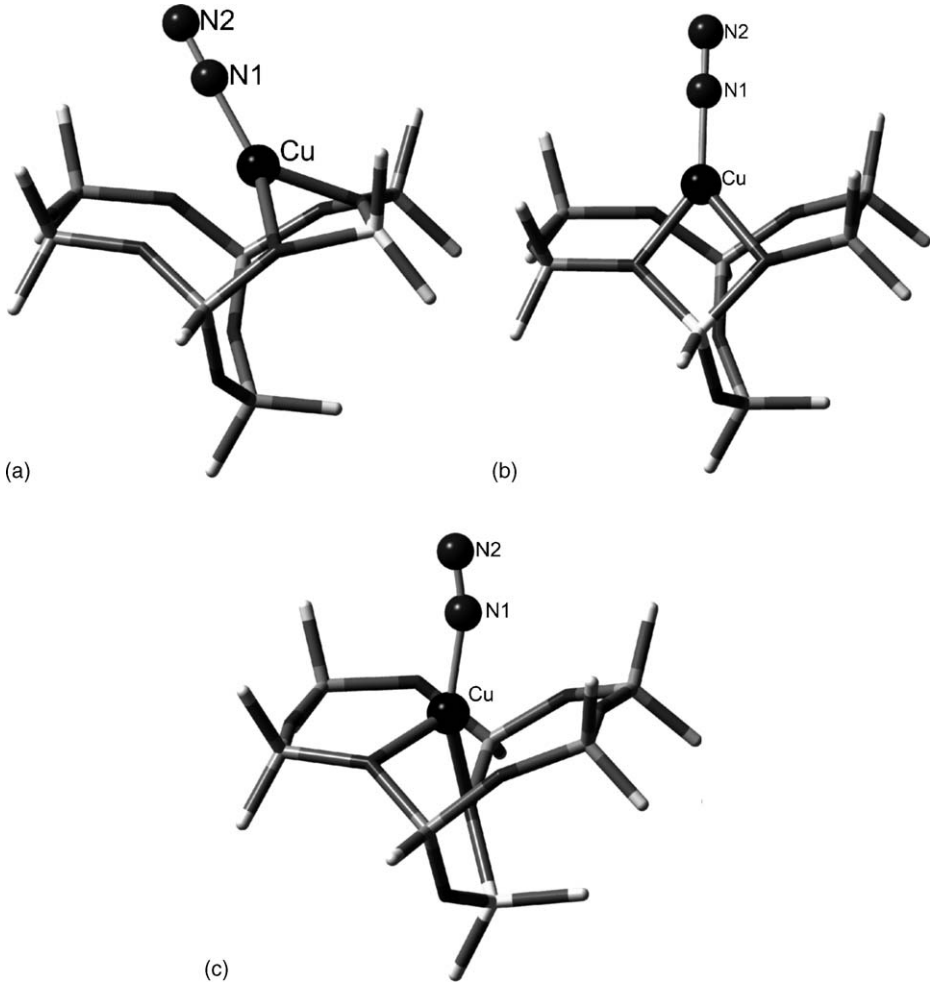

Fig. 12. Adsorption of N_2 by Cu^+ cations stabilized at (a) $Cu^+Z_I^-$, (b) $Cu^+Z_{II}^-$ and (c) $Cu^+Z_{III}^-$ clusters.

3.3. Combined DRIFTS and DFT study of ethane adsorption by Cu^+ cations in the copper modified ZSM-5 zeolite

DRIFT spectra of ethane adsorbed by Cu(I)-ZSM-5 at the relatively high-equilibrium pressures are shown in Fig. 13(a). They contain the following DRIFTS C–H stretching bands: the strong narrow bands at 2974, 2941, 2920 and 2878 cm^{-1}; the weak band at 2738 cm^{-1}; and two weak broad bands with the maxima at 2642 and 2584 cm^{-1}. The former four bands are similar to those previously reported in our study for ethane adsorption by the hydrogen form of ZSM-5 zeolite or for the weak physical ethane adsorption by ZnZSM-5 [34]. Therefore, we also ascribe them to the C_2H_6 molecules weakly perturbed inside the ZSM-5 channels.

One can also see from comparison of the spectra in Fig. 13(a and b) that upon lowering of ethane pressure, the intensities of the bands at 2642 and 2584 cm^{-1} changed quite slightly. At the same time, the intensities of the high-frequency bands from weakly perturbed C_2H_6 very strongly decreased and, instead, several new slightly shifted narrow bands with the maxima at 2989, 2949 and 2892 cm^{-1} become apparent at very low pressures. Thus, the overall DRIFT spectra in Fig. 13(a) correspond to superposition of at least two different forms of weaker and stronger ethane adsorption.

The simultaneous decreasing in intensities of the bands at 2989, 2949 and 2892 cm^{-1} with those of the low-frequency bands at 2642 and 2584 cm^{-1} shows that all of them belong to the same form of ethane adsorption by the univalent copper cations. This form predominates at low pressure and, most likely, the dotted line in Fig. 13(b) represents the individual DRIFT spectra of C–H stretching vibrations of ethane specifically adsorbed by Cu^+ cations.

The appearance of the very strongly red shifted bands in this spectra is most striking. Recently, we also observed the similar very strong batachromic shift by more than 220 cm^{-1} for ν_1C–H stretching vibrations in the DRIFT spectrum of ethane adsorbed by the zinc modified ZSM-5 zeolite [34]. However, adsorption of ethane by the positively charged Zn^{2+} cations also resulted in enormously high intensity of this band in comparison with the other bands from C–H stretching vibrations. It was suggested that this effect is connected with the selective polarization of the corresponding C–H vibrational

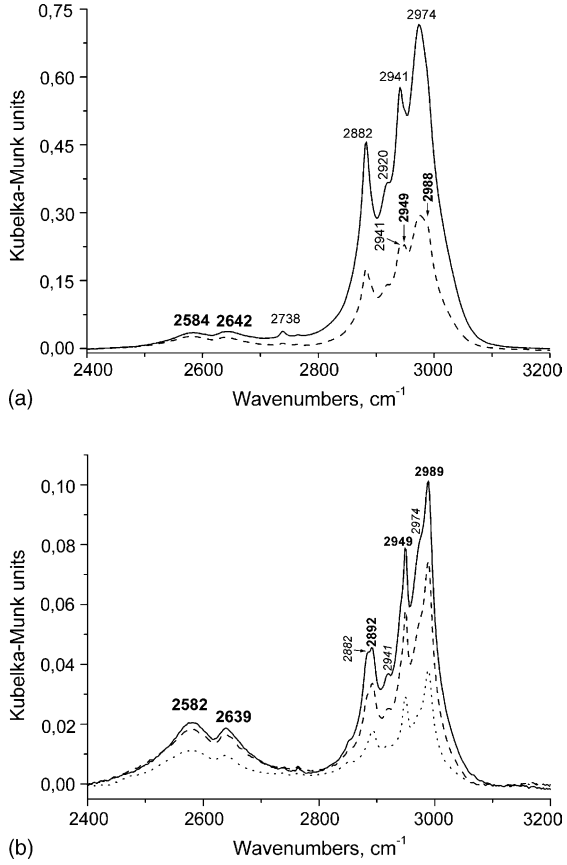

Fig. 13. DRIFT spectra of ethane adsorbed by Cu(I)-ZSM-5 at room temperature and (a) at the relatively high-equilibrium pressures of 200 Pa (—), 133 Pa (- - -) and (b) at low-equilibrium pressures of 13.33 Pa (—), 6.67 Pa (- - -) or 1.33 Pa (· · ·).

mode, which, in turn, led to the heterolytic dissociative adsorption of ethane at elevated temperatures.

In contrast, as one can see from Fig. 13(b), despite of even larger low-frequency shift of the C–H vibrations, the relative intensities of these most strongly red shifted bands is quite low. In addition, the heating of the copper modified sample in ethane atmosphere at elevated temperature up to 673 K did not result in heterolytic dissociative adsorption. Instead such treatment resulted in the strong darkening of the sample that testified reduction of Cu^+ cations into copper metal and made the subsequent DRIFT study of ethane adsorption impossible.

These results and the lower polarizing ability of Cu^+ cations in comparison with the Zn^{2+} cations with the only partially compensated positive charge [18,19] definitely indicate that the unusually strong perturbation of ethane by univalent copper ions has nothing in common with polarization of adsorbed molecules. Instead, very strong low-frequency shifts of C–H stretching vibrations of ethane adsorbed by Cu^+ ions should be explained by some other reasons.

As it was already discussed above, adsorption of dihydrogen by the copper modified ZSM-5 zeolite results in formation of rather strong σ-type $[Cu^+(\eta^2\text{-}H_2)]Z^-$ complexes (by the η^2-structure, we mean two hydrogen atoms bounded to the copper cation). The bonding of H_2 in such complexes results from a combination of the ligand-to-metal electron donation from H_2 σ-orbital to the partially occupied Cu^+ s-orbital combined with the metal-to-ligand back donation from the copper d_π-orbital to the H_2 σ^*-orbital. Both of these interactions lead to the very strong weakening of the H–H bond and, therefore, explain a very strong red shift of the H–H stretching vibrations.

Below we also suggest to explain DRIFT spectra of ethane adsorbed by Cu^+ cations with unusually strongly low-frequency shifted C–H DRIFT bands by formation of the similar σ-complexes. In this connection, it is possible to consider two following η^1 and η^2 alternative structures for ethane adsorption by Cu^+ ions: (Fig. 14). The η^3 structure is not considered due to

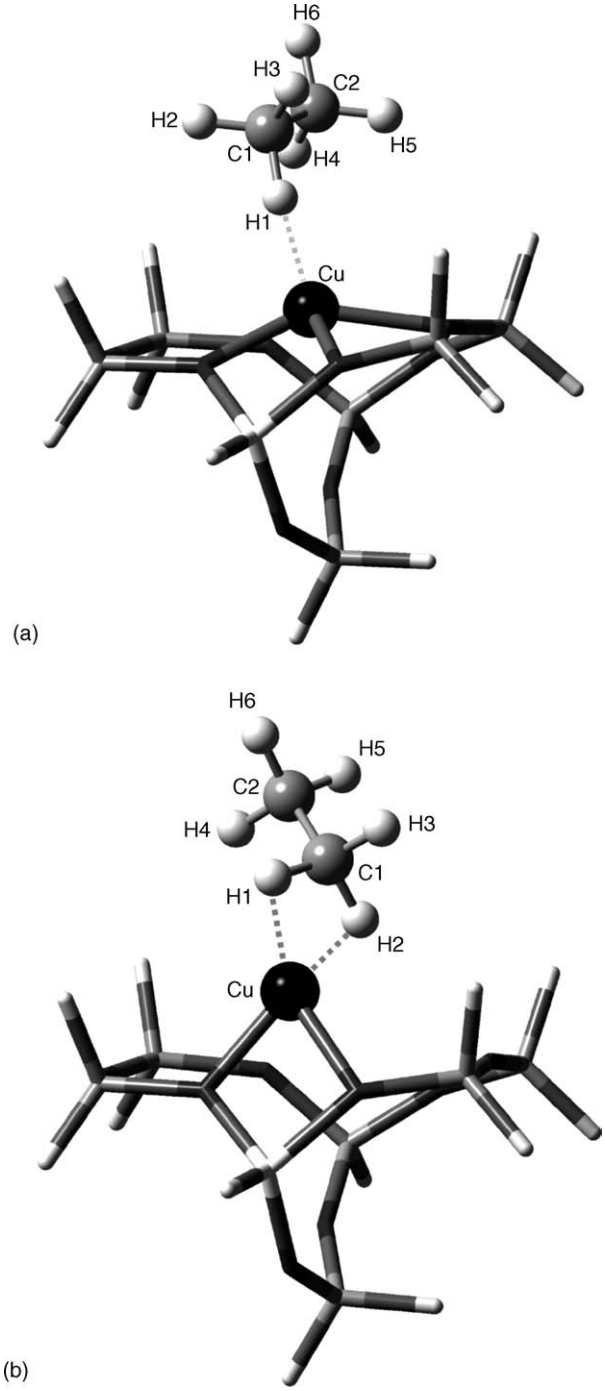

Fig. 14. Adsorption of ethane by $Cu^+Z_{II}^-$ cluster with (a) η^1 and (b) η^2-geometry.

Table 4
Calculated IR frequencies[a] (cm^{-1}) of the C–H stretching vibrations for both the isolated and adsorbed by $Cu^+Z_{II}^-$ cluster ethane molecule, C_2H_6 adsorption energies (kcal/mol), interatomic distances of the C_2H_6–Cu moiety (Å); experimental DRIFTS frequencies of the C–H vibrations of C_2H_6 adsorbed on Cu(I)-ZSM-5

	C_2H_6	η^1-C_2H_6/$Cu^+Z_{II}^-$	η^2-C_2H_6/$Cu^+Z_{II}^-$	C_2H_6/CuZSM-5 (experimental)
ν_7	2973 (70 × 2)[b]	2990 (34)	2990 (19)	2989
		2975 (24)	2981 (15)	n.a.
ν_{10}	2951 (0 × 2)	2965 (14)	2968 (1)	2949
		2932 (14)	2912 (19)	2892
ν_5	2899 (58)	2905 (21)	2652 (16)	2639
ν_1	2897 (0)	2718 (81)	2565 (17)	2582
E_{ads}	–	15.04	22.74	n.a.
l(Cu–H)	–	1.835	1.728/1.752	n.a.
l(C1–H1)	1.095	1.113	1.121	n.a.
l(C1–H2)	1.095	1.094	1.128	n.a.
l(C1–H3)	1.095	1.094	1.092	n.a.
l(C2–H4)	1.095	1.095	1.093	n.a.
l(C2–H5)	1.095	1.094	1.094	n.a.
l(C2–H6)	1.095	1.095	1.094	n.a.
l(C1–C2)	1.530	1.527	1.528	n.a.

[a] Scaling factor equal to 0.952 was used to minimize systematic errors in the calculated frequencies.
[b] The numbers in parentheses correspond to the calculated intensities of the IR bands (km/mol).

only partial removal for the C_{3v} geometry of degeneration of C–H stretching vibrations. Therefore, in contradiction with our experimental results, the corresponding DRIFT spectrum should contain only four IR bands. In contrast, formation of both η^1 and η^2 complexes should result in the stronger lowering of the symmetry of adsorbed ethane from D_{3d} to C_s. One can also suggest that for the η^1-structure the electron donation from σ C–H orbital to the partially occupied s-copper orbital should be less effective due to much lower overlap of the corresponding orbitals. Therefore, the η^2 structure may be favoured.

These expectations were tested by the DFT modelling of C_2H_6 adsorption by the $Cu^+Z_{II}^-$ cluster. The obtained optimized structures of $[Cu^+(\eta^1\text{-}C_2H_6)]Z^-$ and $[Cu^+(\eta^2\text{-}C_2H_6)]Z^-$ complexes are shown in Fig. 14(a and b), respectively, while Table 4 documents the C_2H_6 adsorption energies, the calculated frequencies of C–H stretching vibrations and interatomic distances of the Cu–C_2H_6 moiety. In contrast, η^3-adsorption was not realized, since optimization of geometry resulted in formation of $[Cu^+(\eta^2\text{-}C_2H_6)]Z^-$ complex. The obtained values of adsorption energies for the η^1- and η^2-structures were equal to 15.04 and 22.75 kcal/mol, respectively. As follows from refs. [36,37,44], these values are quite reasonable for the alkane-transition metal complexes. One can also emphasize that formation of the η^2-adsorption complex leads to the very significant changes in geometry of the adsorption site: the Cu^+ ion partially leaves the cationic site, while similar to adsorption of hydrogen, the coordination number of Cu^+ to the lattice oxygen atoms becomes equal to 2. In contrast, formation of the η^1-complex results only in a slight increase of the Cu–O bond lengths (Table 1).

For the η^2-structure, the computed adsorption energy is by about 8 kcal/mol higher than for the η^1 complex. Interaction of two C–H bonds with the Cu^+ cation also leads to the much stronger changes in geometry of the corresponding methyl group and, therefore, results in the stronger low-frequency shifts of the corresponding C–H stretching vibrations. The larger red shift corresponds to symmetric C–H vibration, while the lower shift to the asymmetric vibration of the Cu–C_2H_6 moiety. For both adsorption complexes the C–H bonds involved in the bonding with the Cu^+ ions are considerably longer than those calculated for the free C_2H_6. The rest of C–H bonds of adsorbed ethane are perturbed insignificantly.

Thus, the results of the theoretical modelling are in a reasonably good agreement with the above-discussed experimental data. Indeed, as follows from Table 5, the calculated C–H stretching frequencies for the $[Cu^+(\eta^2\text{-}C_2H_6)]Z^-$ are close to those in the experimentally observed DRIFT spectra. This confirms that the dotted line in Fig. 13(b) really corresponds to the individual spectrum of ethane in the complex with the η^2-geometry. The very weak band at 2734 cm^{-1} could be then ascribed to the η^1-adsorption complexes with the lower adsorption energy.

Despite both the experimental results and theoretical calculations show that ethane adsorption by Cu(I)-ZSM-5 results in a very strong perturbation of two C–H stretching vibrations, the heating of the copper modified sample in the ethane atmosphere at the temperatures up to 673 K did not result in heterolytic dissociative adsorption. This is different from ethane adsorption by ZnZSM-5. In principal, instead, the interaction of C_2H_6 with the very strongly weakened C–H bonds with Cu^+ could result either in the oxidative addition [36] or in reduction of the exchanged copper cations. For Cu^+ the first of these possibilities is, however, very improbable, since formation of the species containing trivalent copper is very exotic. Instead copper is reduced by ethane into zero valence state.

To clarify the nature of the unusually strong perturbation of ethane by the isolated Cu^+ ions at the α-sites, we also performed the NBO analysis for the $[Cu^+(\eta^n\text{-}C_2H_6)]Z^-$ ($n = 1, 2$) adsorption complexes. The obtained orbital-populations and energies of the donor–acceptor interactions between C_2H_6 and

Table 5
Energies of donor–acceptor interactions between C_2H_6 and $Cu^+Z_{II}^-$ (kcal/mol), and NBO population analysis (electrons) for C_2H_6, $Cu^+Z_{II}^-$, η^1-$C_2H_6/Cu^+Z_{II}^-$ and η^2-$C_2H_6/Cu^+Z_{II}^-$ clusters

	Isolated C_2H_6 and $Cu^+Z_{II}^-$	η^1-C_2H_6/ $Cu^+Z_{II}^-$	η^2-C_2H_6/ $Cu^+Z_{II}^-$
$E_{don} = \sigma(C–H) \rightarrow 4s(Cu^+)$	–	4.5	32.5
$E_{back} = 3d(Cu^+) \rightarrow \sigma^*(C–H)$	–	16.5	18.5
Population analysis			
$4s(Cu^+)$	0.18	0.15	0.20
$3d(Cu^+)$	9.86	9.83	9.79
σ(C1–H1)	2.00	1.98	1.96
σ^*(C1–H1)	0.00	0.06	0.05
σ(C1–H2)	2.00	2.00	1.96
σ^*(C1–H2)	0.00	0.00	0.05

Cu^+ are summarized in Table 5. As one can see from this Table, for the η^1-adsorption mode the overlap of the low-occupied Cu^+ s-orbital with C–H σ-orbital of ethane is very strongly influenced by the steric factors. Therefore, the ligand-to-metal donation is very weak (E_{don} = 4.5 kcal/mol). Instead, the strongest interaction is the metal-to-ligand back donation from the copper d_σ-and s-orbitals to the σ^*C–H orbital (E_{back} = 16.5 kcal) (Fig. 15(a)). On the other hand, for $[Cu^+(\eta^2\text{-}C_2H_6)]Z^-$ adsorption complexes both types of the ligand–metal interactions are much stronger (E_{back} = 18.5 kcal/mol and E_{don} = 32.5 kcal/mol). Therefore, the ethane bonding with Cu^+ could be reasonably well described in the similar way as for the $[Cu^+(\eta^2\text{-}H_2)]Z^-$ complexes, i.e. by a synergetic combination of the ligand-to-metal electron donation from C–H σ-orbitals to the low-occupied Cu^+ s-orbital combined with metal-to-ligand back-donation from copper d_π-orbitals to the C–H σ^*-orbitals (Fig. 15(b)). Obviously, both for η^1- and η^2-C_2H_6 complexes each component of such interaction with univalent copper results in a very strong weakening of the C–H bonds contacting the copper ion. However, only formation of η^2-adsorption complex results in an unusually strong red shift of the C–H stretching IR bands of adsorbed ethane, since both the donation and the back-donation in this case are much more effective.

Due to the very low stability, the complexes of transition metals with the light alkanes have been earlier reported only for very specific conditions such as matrix isolation, laser flash photolysis or as intermediates in the reactions of oxidative addition or reductive elimination. The present study shows that the zeolite matrix can substantially promote formation of σ-ethane complexes with Cu^+ ions. The search for the complexes of paraffins with other low-valence transition metal ions stabilized in zeolites is therefore very promising.

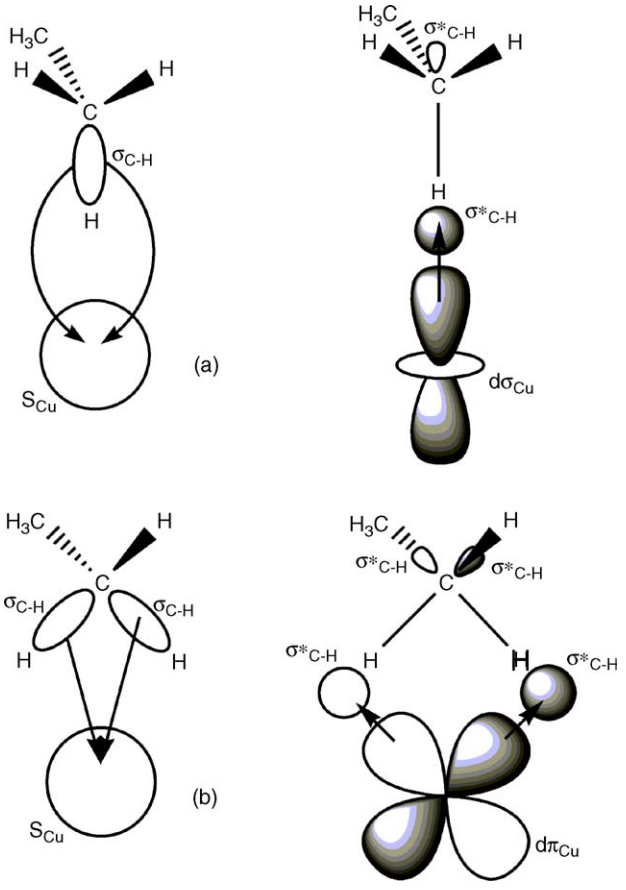

Fig. 15. Schematic representation of donor–acceptor interactions between the C_2H_6 molecule and the Cu^+ cation of the (a) $[Cu^+(\eta^1\text{-}C_2H_6)]Z^-$ and (b) $[Cu^+(\eta^2\text{-}C_2H_6)]Z^-$ adsorption complexes.

4. Conclusion

The summary of the above-discussed experimental data indicates that independently on the preparation method Cu^+ containing ZSM-5 zeolites exhibit a very similar adsorption properties. Adsorption of H_2 by a part of Cu^+ ions in CuZSM-5 results in a very strong perturbation of adsorbed molecules, which is evident from the very strong low-frequency shift of the corresponding H–H stretching frequencies. The Cu^+ sites strongly interacting with adsorbed hydrogen are the same as for the strong N_2 adsorption. In addition, at least two different Cu^+ sites were discriminated by DRIFTS of adsorbed H_2. It was also shown that the number of Cu^+ ions strongly adsorbing molecular hydrogen is somewhat less than the number of sites of the strong N_2 adsorption. This could be explained by different surrounding of Cu^+ at the cation sites, which results in different electronic properties of the exchanged cations. The DFT modelling of H_2 adsorption by Cu^+ cations at α-site of ZSM-5 zeolite allowed more convincing assignment of the experimental IR data.

It was also shown that adsorption of ethane by ZSM-5 zeolite modified with Cu^+ ions results in very strong perturbation of adsorbed molecules, which leads to the very large red-shift of C–H stretching bands that has never been observed before for ethane adsorbed on any cationic form of zeolites or oxide. It was concluded that such unusual properties of adsorbed C_2H_6 molecules resulted from formation of a rather strong σ-type adsorption complexes with the exchanged univalent copper cations. These results could be considered as the first direct DRIFTS observation of stable alkane transition metal complexes.

References

[1] M. Iwamoto, S. Yokoo, K. Sakai, S. Kagawa, J. Chem. Soc. 77 (1981) 1629.
[2] G. Centi, S. Perathoner, Appl. Catal. A 132 (1995) 179.
[3] M. Shelef, Chem. Rev. 95 (1995) 209.
[4] G. Spoto, S. Bordiga, G. Ricchiardi, D. Scarano, A. Zecchina, F. Geobaldo, J. Chem. Soc. Faraday Trans. 91 (1995) 3285.
[5] Y. Kuroda, R. Kumashiro, A. Itadani, M. Nagao, H. Kobayashi, Phys. Chem. Chem. Phys. 3 (2001) 1383.
[6] R. Kumashiro, Y. Kuroda, M. Nagao, J. Phys. Chem. 103 (1999) 89.
[7] C. Lamberti, S. Bordiga, M. Salvalaggio, G. Spoto, A. Zecchina, F. Geobaldo, G. Vlaic, M. Bellatreccia, J. Phys. Chem. B 101 (1997) 344.
[8] G. Spoto, A. Zecchina, S. Bordiga, G. Ricchiardi, G. Martra, Appl. Catal. B 3 (1994) 151.
[9] V. Bolis, A. Barbaglia, S. Bordiga, C. Lamberti, A. Zeccina, J. Phys. Chem. B 108 (2004) 9970.
[10] L.M. Kustov, V.B. Kazansky, J. Chem. Soc. Faraday Trans. 87 (1991) 2675.
[11] A.Yu. Khodakov, L.M. Kustov, V.B. Kazansky, C. Williams, J. Chem. Soc. Faraday Trans. 88 (1992) 3251.
[12] K. Beck, H. Pfeifer, S. Staudte, J. Chem. Soc. Faraday Trans. 89 (1993) 3995.
[13] V.B. Kazansky, V.Yu. Borovkov, H.G. Karge, J. Chem. Soc. Faraday Trans. 93 (1997) 1843.
[14] V.B. Kazansky, J. Mol. Catal. A: Chem. 141 (1999) 83.
[15] V.B. Kazansky, V.Yu. Borovkov, A.I. Serykh, R.A. van Santen, P.J. Stobbelaar, Phys. Chem. Chem. Phys. 1 (1999) 2881.
[16] V.B. Kazansky, A.I. Serykh, A.T. Bell, Catal. Lett. 83 (2002) 191.
[17] V.B. Kazansky, J. Catal. 216 (2003) 966.
[18] V.B. Kazansky, A.I. Serykh, Phys. Chem. Chem. Phys. 6 (2004) 3760.
[19] V. Kazansky, A. Serykh, Microporous Mesoporous Mater. 70 (2004) 151.
[20] A.I. Serykh, V.B. Kazansky, Phys. Chem. Chem. Phys. 6 (2004) 5250.
[21] V.B. Kazansky, A.I. Serykh, Catal. Lett. 98 (2004) 77.
[22] X. Solans-Monfort, V. Branchadell, M. Sodupe, C.M. Zicovich-Wilson, E. Gribov, G. Spoto, C. Busco, P. Ugliengo, J. Phys. Chem. B 108 (2004) 8278.
[23] G. Spoto, E. Gribov, S. Bordiga, C. Lamberti, G. Ricchiardi, D. Scarano, A. Zecchina, Chem. Commun. (2004) 2768.
[24] G.J. Kubas, R.R. Ryan, B.I. Swanson, P.J. Vergamini, H.J. Wasserman, J. Am. Chem. Soc. 106 (1984) 451.
[25] G.J. Kubas, Acc. Chem. Res. 21 (1988) 120.
[26] R.H. Grabtree, Acc. Chem. Res. 23 (1990) 95.
[27] D.M. Heinekey, W.J. Ordham Jr., Chem. Rev. 93 (1993) 913.
[28] R.H. Morris, Can. J. Chem. 74 (1996) 1907.
[29] M.A. Esteruelas, L.A. Oro, Chem. Rev. 98 (1998) 577.
[30] G.S. McGrady, G. Guilera, Chem. Soc. Rev. 32 (2003) 383.
[31] D.M. Heinekey, A. Lledos, J.M. Lluch, Chem. Soc. Rev. 33 (2004) 175.
[32] P. Buskens, D. Giunta, W. Leitner, Inorg. Chem. Acta 357 (2004) 1969.
[33] V.B. Kazansky, A.I. Serykh, E.A. Pidko, J. Catal. 225 (2004) 369.
[34] V.B. Kazansky, E.A. Pidko, J. Phys. Chem. B 109 (2005) 2103.
[35] A.Yu. Khodakov, L.M. Kustov, V.B. Kazansky, C. Williams, J. Chem. Soc. Faraday Trans. 89 (1993) 1393.
[36] R.H. Crabtree, Chem. Rev. 95 (1995) 987.
[37] C.H. Hall, R.N. Perutz, Chem. Rev. 96 (1996) 3125.
[38] M.A. Graham, R.N. Perutz, M. Poliakoff, J.J. Turner, J. Organomet. Chem. 97 (1972) 4791.
[39] R.N. Perutz, J.J. Turner, J. Am. Chem. Soc. 97 (1975) 4791.
[40] J.M. Kelly, H. Hermann, E.K. Von Gustorf, J. Chem. Soc. Chem. Commun. (1973) 105.
[41] G.I. Childs, D.C. Crills, X.Z. Sun, M.W. George, Pure Appl. Chem. 73 (2001) 443.
[42] C.E. Brown, Y. Ishikawa, P.A. Hackett, P.M. Rayner, J. Am. Chem. Soc. 112 (1990) 2530.
[43] W.D. Jones, Acc. Chem. Res. 36 (2003) 140.
[44] V.D. Makhaev, Uspekhi Khimii (Russ.) 72 (2003) 287.
[45] M.J. Frisch, G.W. Trucks, H.B. Schlegel, G.E. Scuseria, M.A. Robb, J.R. Cheeseman, V.G. Zakrzewski, J.A. Montgomery Jr., R.E. Stratmann, J.C. Burant, S. Dapprich, J.M. Millam, A.D. Daniels, K.N. Kudin, M.C. Strain, O. Farkas, J. Tomasi, V. Barone, M. Cossi, R. Cammi, B. Mennucci, C. Pomelli, C. Adamo, S. Clifford, J. Ochterski, G.A. Petersson, P.Y. Ayala, Q. Cui, K. Morokuma, D.K. Malick, A.D. Rabuck, K. Raghavachari, J.B. Foresman, J. Cioslowski, J.V. Ortiz, A.G. Baboul, B.B. Stefanov, G. Liu, A. Liashenko, P. Piskorz, I. Komaromi, R. Gomperts, R.L. Martin, D.J. Fox, T. Keith, M.A. Al-Laham, C.Y. Peng, A. Nanayakkara, M. Challacombe, P.M.W. Gill, B. Johnson, W. Chen, M.W. Wong, J.L. Andres, C. Gonzalez, M. Head-Gordon, E.S. Replogle, J.A. Pople, Gaussian 98 Revision A.9, Gaussian, Inc., Pittsburgh, PA, 1998.
[46] A.D. Becke, Phys. Rev. A38 (1988) 3098;
A.D. Becke, J. Chem. Phys. 98 (1993) 1372;
A.D. Becke, J. Chem. Phys. 98 (1993) 5648.
[47] J. Backer, M. Muir, J. Andzelm, A. Scheiner, Chemical applications of density-functional theory, in: B.B. Laird, R.B. Ross, T. Ziegler (Eds.), ACS Symposium Series, vol. 629, American Chemical Society, Washington DC, 1996.
[48] J. Dedecek, B. Wichterlova, Phys. Chem. Chem. Phys. 1 (1999) 629.
[49] D. Nachtigallova, P. Nachtigall, M. Sierka, J. Sauer, PCCP 1 (1999) 2019.
[50] D.H. Olson, G.T. Kokotailo, S.L. Lawton, W.M. Meier, J. Chem. Phys. 85 (1981) 2238.
[51] A.A. Shubin, G.M. Zhidomirov, V.B. Kazansky, R.A. van Santen, Catal. Lett. 90 (2003) 137.
[52] A.A. Reed, L.A. Curtiss, F. Weinhold, Chem. Rev. 88 (1988) 899.
[53] Y. Kuroda, Y. Yoshikawa, S. Konno, H. Hamano, H. Maeda, R. Kumashiro, M. Nagao, J. Phys. Chem. 99 (1995) 10621.
[54] G.T. Palomino, P. Fisicaro, S. Bordiga, A. Zecchina, E. Giamello, C. Lamberti, J. Phys. Chem. B 104 (2000) 4064.
[55] F.X. Llabrés i Xamena, P. Fisicaro, G. Berlier, A. Zecchina, G.T. Palomino, C. Prestipino, S. Bordiga, E. Giamello, C. Lamberti, J. Phys. Chem. B 107 (2003) 7036.
[56] H.S. Plitt, M.R. Bär, R. Ahlrichs, H. Schnöckel, Angew. Chem. Int. Ed. Engl. 30 (1991) 832.